
CASTLE: Regularization via Auxiliary Causal Graph Discovery

Trent Kyono*

University of California, Los Angeles
tmkyono@gmail.com

Yao Zhang*

University of Cambridge
yz555@cam.ac.uk

Mihaela van der Schaar

University of Cambridge
University of California, Los Angeles
The Alan Turing Institute
mv472@cam.ac.uk

Abstract

Regularization improves generalization of supervised models to out-of-sample data. Prior works have shown that prediction in the causal direction (effect from cause) results in lower testing error than the anti-causal direction. However, existing regularization methods are agnostic of causality. We introduce Causal Structure Learning (CASTLE) regularization and propose to regularize a neural network by jointly learning the causal relationships between variables. CASTLE learns the causal directed acyclical graph (DAG) as an adjacency matrix embedded in the neural network’s input layers, thereby facilitating the discovery of optimal predictors. Furthermore, CASTLE efficiently reconstructs only the features in the causal DAG that have a causal neighbor, whereas reconstruction-based regularizers suboptimally reconstruct all input features. We provide a theoretical generalization bound for our approach and conduct experiments on a plethora of synthetic and real publicly available datasets demonstrating that CASTLE consistently leads to better out-of-sample predictions as compared to other popular benchmark regularizers.

1 Introduction

A primary concern of machine learning, and deep learning in particular, is generalization performance on out-of-sample data. Over-parameterized deep networks efficiently learn complex models and are, therefore, susceptible to overfit to training data. Common regularization techniques to mitigate overfitting include data augmentation [1, 2], dropout [3, 4, 5], adversarial training [6], label smoothing [7], and layer-wise strategies [8, 9, 10] to name a few. However, these methods are agnostic of the causal relationships between variables limiting their potential to identify optimal predictors based on graphical topology, such as the causal parents of the target variable. An alternative approach to regularization leverages supervised reconstruction, which has been proven theoretically and demonstrated empirically to improve generalization performance by obligating hidden bottleneck layers to reconstruct input features [11, 12]. However, supervised auto-encoders suboptimally reconstruct all features, including those without causal neighbors, i.e., adjacent cause or effect nodes. Naively reconstructing these variables does not improve regularization and representation learning for the predictive model. In some cases, it may be harmful to generalization performance, e.g., reconstructing a random noise variable.

*Equal contribution

Although causality has been a topic of research for decades, only recently has cause and effect relationships been incorporated into machine learning methodologies and research. Recently, researchers at the confluence of machine learning and causal modeling have advanced causal discovery [13, 14], causal inference [15, 16], model explainability [17], domain adaptation [18, 19, 20] and transfer learning [21] among countless others. The existing synergy between these two disciplines has been recognized for some time [22], and recent work suggests that causality can improve and complement machine learning regularization [23, 24, 25]. Furthermore, many recent causal works have demonstrated and acknowledged the optimality of predicting in the causal direction, i.e., predicting effect from cause, which results in less test error than predicting in the anti-causal direction [21, 26, 27, 28].

Contributions. In this work, we introduce a novel regularization method called CASTLE (CAusal STructure LEarning) regularization. CASTLE regularization uses causal graph discovery as an auxiliary task when training a supervised model to improve the generalization performance of the primary prediction task. Specifically, CASTLE learns the causal directed acyclical graph (DAG) under continuous optimization as an adjacency matrix embedded in a feed-forward neural network’s input layers. By jointly learning the causal graph, CASTLE can surpass the benefits provided by feature selection regularizers by identifying optimal predictors, such as the target variable’s causal parents. Additionally, CASTLE further improves upon auto-encoder-based regularization [12] by reconstructing only the input features that have neighbors (adjacent nodes) in the causal graph. Regularization of a predictive model to satisfy the causal relationships among feature and target variables effectively guide the model towards the direction of better out-of-sample generalization guarantees. We provide a theoretical generalization bound for CASTLE and demonstrate improved performance against a variety of benchmark methods on a plethora of real and synthetic datasets.

2 Related Works

We compare to the related work in the simplest supervised learning setting where we desire learning a function from some features \mathbf{X} to a target variable Y given some data of the variables \mathbf{X} and Y to improve out-of-sample generalization within the same distribution. This is a significant departure from the branches of machine learning algorithms, such as in semi-supervised learning and domain adaptation, where the regularizer is constructed with information other than variables \mathbf{X} and Y .

Table 1: Comparison of related works.

METHOD	FEAT. SEL.	STRUCT. LEARNING	CAUSAL PRED.	TARGET SEL.
CAPACITY-BASED	✓	✗	✗	✗
SAE	✗	✓	✗	✗
CASTLE	✓	✓	✓	✓

Regularization controls model complexity and mitigates overfitting. ℓ_1 [29] and ℓ_2 [30] regularization are commonly used regularization approaches where the former is used when a sparse model is preferred. For deep neural networks, dropout regularization [3, 4, 5] has been shown to be superior in practice to ℓ_p regularization techniques. Other capacity-based regularization techniques commonly used in practice include early stopping [31], parameter sharing [31], gradient clipping [32], batch normalization [33], data augmentation [2], weight noise [34], and MixUp [35] to name a few. Norm-based regularizers with sparsity, e.g. Lasso [29], are used to guide feature selection for supervised models. The work of [12] on supervised auto-encoders (SAE) theoretically and empirically shows that adding a reconstruction loss of the input features functions as a regularizer for predictive models. However, this method does not select which features to reconstruct and therefore suffers performance degradation when tasked to reconstruct features that are noise or unrelated to the target variables.

Two existing works [25, 23] attempt to draw the connection between causality and regularization. Based on an analogy between overfitting and confounding in linear models, [25] proposed a method to determine the regularization hyperparameter in linear Ridge or Lasso regression models by estimating the strength of confounding. [23] use causality detectors [36, 27] to weight a sparsity regularizer, e.g. ℓ_1 , for performing non-linear causality analysis and generating multivariate causal hypotheses. Neither of the works has the same objective as us — improving the generalization performance of supervised learning models, nor do they overlap methodologically by using causal DAG discovery.

Causal discovery is an NP-hard problem that requires a brute-force search through a non-convex combinatorial search space, limiting the existing algorithms to reaching global optima for only small problems. Recent approaches have successfully accelerated these methods by using a novel

acyclicity constraint and formulating the causal discovery problem as a continuous optimization over real matrices (avoiding combinatorial search) in the linear [37] and nonlinear [38, 39] cases. CASTLE incorporates these recent causal discovery approaches of [37, 38] to improve regularization for prediction problems in general.

As shown in Table 1, CASTLE regularization provides two additional benefits: causal prediction and target selection. First, CASTLE identifies causal predictors (e.g., causal parents if they exist) rather than correlated features. Furthermore, CASTLE improves upon reconstruction regularization by only reconstructing features that have neighbors in the underlying DAG. We refer to this advantage as “target selection”. Collectively these benefits contribute to the improved generalization of CASTLE. Next we introduce our notation (Section 3.1) and provide more details of these benefits (Section 3.2).

3 Methodology

In this section, we provide a problem formulation with causal preliminaries for CASTLE. Then we provide a motivational discussion, regularizer methodology, and generalization theory for CASTLE.

3.1 Problem Formulation

In the standard supervised learning setting, we denote the input feature variables and target variable, by $\mathbf{X} = [X_1, \dots, X_d] \in \mathcal{X}$ and $Y \in \mathcal{Y}$, respectively, where $\mathcal{X} \subseteq \mathbb{R}^d$ is a d -dimensional feature space and $\mathcal{Y} \subseteq \mathbb{R}$ is a one-dimensional target space. Let $P_{\mathbf{X}, Y}$ denote the joint distribution of the features and target. Let $[N]$ denote the set $\{1, \dots, N\}$. We observe a dataset, $\mathcal{D} = \{(\mathbf{X}_i, Y_i), i \in [N]\}$, consisting of N i.i.d. samples drawn from $P_{\mathbf{X}, Y}$. The goal of a supervised learning algorithm \mathcal{A} is to find a predictive model, $f_Y : \mathcal{X} \rightarrow \mathcal{Y}$, in a hypothesis space \mathcal{H} that can explain the association between the features and the target variable. In the learning algorithm \mathcal{A} , the predictive model \hat{f}_Y is trained on a finite number of samples in \mathcal{D} , to predict well on the out-of-sample data generated from the same distribution $P_{\mathbf{X}, Y}$. However, overfitting, a mismatch between training and testing performance of \hat{f}_Y , can occur if the hypothesis space \mathcal{H} is too complex and the training data fails to represent the underlying distribution $P_{\mathbf{X}, Y}$. This motivates the usage of regularization to reduce the hypothesis space’s complexity \mathcal{H} so that the learning algorithm \mathcal{A} will only find the desired function to explain the data. Assumptions of the underlying distribution dictate regularization choice. For example, if we believe only a subset of features is associated with the label Y , then ℓ_1 regularization [29] can be beneficial in creating sparsity for feature selection.

CASTLE regularization is based on the assumption that a causal DAG exists among the input features and target variable. In the causal framework of [40], a causal structure of a set of variables \mathbf{X} is a DAG in which each vertex $v \in V$ corresponds to a distinct element in \mathbf{X} , and each edge $e \in E$ represents direct functional relationships between two neighboring variables. Formally, we assume the variables in our dataset satisfy a nonparametric structural equation model (NPSEM) as defined in Definition 1. The word “nonparametric” means we do not make any assumption on the underlying functions f_i in the NPSEM. In this work, we characterize optimal learning by a predictive model as discovering the function $Y = f_Y(\text{Pa}(Y), u_Y)$ in NPSEM [40].

Definition 1. (NPSEMs) Given a DAG $\mathcal{G} = (V = [d + 1], E)$, the random variables $\tilde{\mathbf{X}} = [Y, \mathbf{X}]$ satisfy a NPSEM if

$$X_i = f_i(\text{Pa}(X_i), u_i), i \in [d + 1],$$

where $\text{Pa}(i)$ is the parents (direct causes) of X_i in \mathcal{G} and $\mathbf{u}_{[d+1]}$ are some random noise variables.

3.2 Why CASTLE regularization matters

We now present a graphical example to explain the two benefits of CASTLE mentioned in Section 2, causal prediction and target selection. Consider Figure 1 where we are given nine feature variables X_1, \dots, X_9 and a target variable Y .

Causal Prediction. The target variable Y is generated by a function $f_Y(\text{Pa}(Y), u_Y)$ from Definition 1 where the parents of Y are $\text{Pa}(Y) = \{X_2, X_3\}$. In CASTLE regularization, we train a predictive model \hat{f}_Y jointly with learning the DAG among \mathbf{X} and Y . The features that the model uses to predict Y are the causal parents of Y in the learned DAG. Such a model is sample efficient in uncovering the

true function $f_Y(\text{Pa}(Y), u_Y)$ and generalizes well on the out-of-sample data. Our theoretical analysis in Section 3.4 validates this advantage when there exists a DAG structure among the variables \mathbf{X} and Y . However, there may exist other variables that predict Y more accurately than the causal parents $\text{Pa}(Y)$. For example, if the function from Y to X_8 is a one-to-one linear mapping, we can predict Y trivially from the feature X_8 . In our objective function introduced later, the prediction loss of Y will be weighted higher than the causal regularizer. Among the predictive models with a similar prediction loss of Y , our objective function still prefers to use the model, which minimizes the causal regularizer and uses the causal parents. However, it would favor the easier predictor if one exists and gives a much lower prediction loss of Y . In this case, the learned DAG may differ from the true DAG, but we reiterate that we are focused on the problem of generalization rather than causal discovery.

Target Selection. Consider the variables X_5 , X_6 and X_7 which share parents (X_2 and X_3) with Y in Figure 1. The functions $X_5 = f_5(X_2, u_5)$, $X_6 = f_6(X_3, u_6)$, and $X_7 = f_7(X_3, u_7)$ may have some learnable similarity (e.g. basis functions and representations) with $Y = f_Y(X_2, X_3, u_Y)$, that we can exploit by training a shared predictive model of Y with the auxiliary task of predicting X_5 , X_6 and X_7 . From the causal graph topology, CASTLE discovers the optimal features that should act as the auxiliary task for learning f_Y . CASTLE learns the related functions jointly in a shared model, which is proven to improve the generalization performance of predicting Y by learning shared basis functions and representations [41].

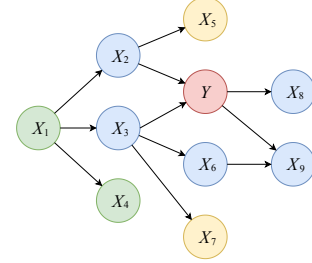


Figure 1: Example DAG.

3.3 CASTLE regularization

Let $\tilde{\mathcal{X}} = \mathcal{Y} \times \mathcal{X}$ denote the data space, $P_{(\mathbf{X}, Y)} = P_{\tilde{\mathbf{X}}}$ the data distribution, and $\|\cdot\|_F$ the Frobenius norm. We define random variables $\tilde{\mathbf{X}} = [\tilde{X}_1, \tilde{X}_2, \dots, \tilde{X}_{d+1}] := [Y, X_1, \dots, X_d] \in \tilde{\mathcal{X}}$. Let $\mathbf{X} = [\mathbf{X}_1, \dots, \mathbf{X}_d]$ denote the $N \times d$ input data matrix, \mathbf{Y} the N -dimensional label vector, $\tilde{\mathbf{X}} = [\mathbf{Y}, \mathbf{X}]$ the $N \times (d+1)$ matrix that contains data of all the variables in the DAG.

To facilitate exposition, we first introduce CASTLE in the linear setting. Here, the parameters are a $(d+1) \times (d+1)$ adjacency matrix \mathbf{W} with zero in the diagonal. The objective function is given as

$$\hat{\mathbf{W}} \in \min_{\mathbf{W}} \frac{1}{N} \|\mathbf{Y} - \tilde{\mathbf{X}} \mathbf{W}_{:,1}\|^2 + \lambda \mathcal{R}_{\text{DAG}}(\tilde{\mathbf{X}}, \mathbf{W}) \quad (1)$$

where $\mathbf{W}_{:,1}$ is the first column of \mathbf{W} . We define the DAG regularization loss $\mathcal{R}_{\text{DAG}}(\tilde{\mathbf{X}}, \mathbf{W})$ as

$$\mathcal{R}_{\text{DAG}}(\tilde{\mathbf{X}}, \mathbf{W}) = \mathcal{L}_{\mathbf{W}} + \mathcal{R}_{\mathbf{W}} + \beta \mathcal{V}_{\mathbf{W}}. \quad (2)$$

where $\mathcal{L}_{\mathbf{W}} = \frac{1}{N} \|\tilde{\mathbf{X}} - \tilde{\mathbf{X}} \mathbf{W}\|_F^2$, $\mathcal{R}_{\mathbf{W}} = (\text{Tr}(e^{\mathbf{W} \odot \mathbf{W}}) - d - 1)^2$, $\mathcal{V}_{\mathbf{W}}$ is the ℓ_1 norm of \mathbf{W} , \odot is the Hadamard product, and $e^{\mathbf{M}}$ is the matrix exponential of \mathbf{M} . The DAG loss $\mathcal{R}_{\text{DAG}}(\tilde{\mathbf{X}}, \mathbf{W})$ is introduced in [37] for learning linear DAG by continuous optimization. Here we use it as the regularizer for our linear regression model $\mathbf{Y} = \tilde{\mathbf{X}} \mathbf{W}_{:,1} + \epsilon$. From Theorem 1 in [37], we know the graph given by \mathbf{W} is a DAG if and only if $\mathcal{R}_{\mathbf{W}} = 0$. The prediction $\hat{\mathbf{Y}} = \tilde{\mathbf{X}} \mathbf{W}_{:,1}$ is the projection of \mathbf{Y} onto the parents of Y in the learned DAG. This increases the stability of linear regression when issues pertaining to collinearity or multicollinearity among the input features appear.

Continuous optimization for learning nonparametric causal DAGs has been proposed in the prior work by [38]. In a similar manner, we also adapt CASTLE to nonlinear cases. Suppose the predictive model for Y and the function generating each feature X_k in the causal DAG are parameterized by an M -layer feed-forward neural network $f_{\Theta} : \tilde{\mathcal{X}} \rightarrow \tilde{\mathcal{X}}$ with ReLU activations and layer size h . Figure 2 shows the network architecture of f_{Θ} . This joint network can be instantiated as a $d+1$ sub-network f_k with shared hidden layers, where f_k is responsible for reconstructing the feature \tilde{X}_k . We let \mathbf{W}_1^k denote the $h \times (d+1)$ weight matrix in the input layer of f_k , $k \in [d+1]$. We set the k -th column of \mathbf{W}_1^k to zero such that f_k does not utilize \tilde{X}_k in its prediction of \tilde{X}_k . We let \mathbf{W}_m , $m = 2, \dots, M-1$ denote the weight matrices in the network's shared hidden layers, and $\mathbf{W}_M = [\mathbf{W}_M^1, \dots, \mathbf{W}_M^{d+1}]$ denotes the $h \times (d+1)$ weight matrix in the output layer. Explicitly, we define the sub-network f_k as

$$f_k(\tilde{\mathbf{X}}) = \phi(\dots \phi(\phi(\tilde{\mathbf{X}} \mathbf{W}_1^k) \mathbf{W}_2) \dots \mathbf{W}_{M-1}) \mathbf{W}_M^k, \quad (3)$$

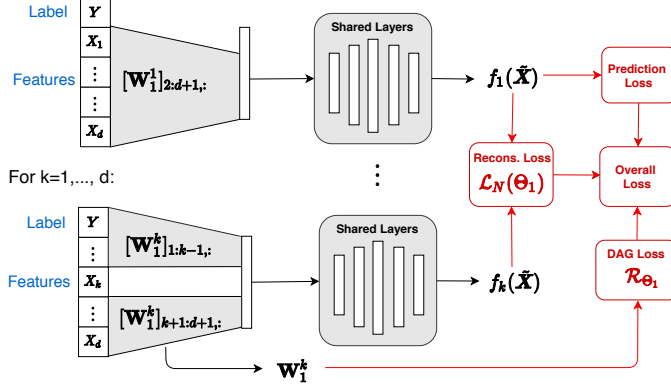


Figure 2: Schematic of CASTLE regularization. Our goal is to have the following tasks: (1) a prediction of a target variable Y , and (2) the discovered causal DAG for input features $\tilde{\mathbf{X}}$ and Y .

where $\phi(\cdot)$ is the ReLU activation function. The function f_{Θ} is given as $f_{\Theta}(\tilde{\mathbf{X}}) = [f_1(\tilde{\mathbf{X}}), \dots, f_{d+1}(\tilde{\mathbf{X}})]$. Let $f_{\Theta}(\tilde{\mathbf{X}})$ denote the prediction for the N samples matrix $\tilde{\mathbf{X}}$ where $[f_{\Theta}(\tilde{\mathbf{X}})]_{i,k} = f_k(\tilde{\mathbf{X}}_i)$, $i \in [N]$ and $k \in [d+1]$. All network parameters are collected into sets as

$$\Theta_1 = \{\mathbf{W}_1^k\}_{k=1}^{d+1}, \quad \Theta = \Theta_1 \cup \{\mathbf{W}_m\}_{k=2}^M \quad (4)$$

The training objective function of f_{Θ} is

$$\Theta \in \min_{\Theta} \frac{1}{N} \|\mathbf{Y} - [f_{\Theta}(\tilde{\mathbf{X}})]_{:,1}\|^2 + \lambda \mathcal{R}_{\text{DAG}}(\tilde{\mathbf{X}}, f_{\Theta}). \quad (5)$$

The DAG loss $\mathcal{R}_{\text{DAG}}(\tilde{\mathbf{X}}, f_{\Theta})$ is given as

$$\mathcal{R}_{\text{DAG}}(\tilde{\mathbf{X}}, f_{\Theta}) = \mathcal{L}_N(f_{\Theta}) + \mathcal{R}_{\Theta_1} + \beta \mathcal{V}_{\Theta_1}. \quad (6)$$

Because the k -th column of the input weight matrix \mathbf{W}_1^k is set to zero, $\mathcal{L}_N(f_{\Theta}) = \frac{1}{N} \|\tilde{\mathbf{X}} - f_{\Theta}(\tilde{\mathbf{X}})\|_F^2$ differs from the standard reconstruction loss in auto-encoders (e.g. SAE) by only allowing the model to reconstruct each feature and target variable from the others. In contrast, auto-encoders reconstruct each feature using all the features including itself. \mathcal{V}_{Θ_1} is the ℓ_1 norm of the weight matrices \mathbf{W}_1^k in Θ_1 , and the term \mathcal{R}_{Θ_1} is given as,

$$\mathcal{R}_{\Theta_1} = (\text{Tr}(e^{\mathbf{M} \odot \mathbf{M}}) - d - 1)^2 \quad (7)$$

where \mathbf{M} is a $(d+1) \times (d+1)$ matrix such that $[\mathbf{M}]_{k,j}$ is the ℓ_2 -norm of the k -th row of the matrix \mathbf{W}_1^j . When the acyclicity loss \mathcal{R}_{Θ_1} is minimized, the sub-networks f_1, \dots, f_{d+1} forms a DAG among the variables; \mathcal{R}_{Θ_1} obligates the sub-networks to reconstruct only the input features that have neighbors (adjacent nodes) in the learned DAG. We note that converting the nonlinear version of CASTLE into a linear form can be accomplished by removing all the hidden layers and output layers and setting the dimension h of the input weight matrices to be 1 in (3), i.e., $f_k(\tilde{\mathbf{X}}) = \tilde{\mathbf{X}} \mathbf{W}_1^k$ and $f_{\Theta}(\tilde{\mathbf{X}}) = [\tilde{\mathbf{X}} \mathbf{W}_1^1, \dots, \tilde{\mathbf{X}} \mathbf{W}_1^{d+1}] = \tilde{\mathbf{X}} \mathbf{W}$, which is the linear model in (1-2).

Managing computational complexity. If the number of features is large, it is computationally expensive to train all the sub-networks simultaneously. We can mitigate this by sub-sampling. At each iteration of gradient descent, we randomly sample a subset of features to reconstruct and only minimize the prediction loss and reconstruction loss on these sub-sampled features. Note that we do not have a hidden confounders issue here, since Y and the sub-sampled features are predicted by all the features except itself. The sparsity DAG constraint on the weight matrices is unchanged at each iteration. In this case, we keep the training complexity per iteration at a manageable level approximately around the computational time and space complexity of training a few networks jointly. We include experiments on CASTLE scalability with respect to input feature size in Appendix C.

3.4 Generalization bound for CASTLE regularization

In this section, we analyze theoretically why CASTLE regularization can improve the generalization performance by introducing a generalization bound for our model in Figure 2. Our bound is based

on the PAC-Bayesian learning theory in [42, 43, 44]. Here, we re-interpret the DAG regularizer as a special prior or assumption on the input weight matrices of our model and use existing PAC-Bayes theory to prove the generalization of our algorithm. Traditionally, PAC-Bayes bounds are only applied to randomized models, such as Bayesian or Gibbs classifiers. Here, our bound is applied to our deterministic model by using the recent derandomization formalism from [45, 46]. We acknowledge and note that developing tighter and non-vacuous generalization bounds for deep neural networks is still a challenging and evolving topic in learning theory. The bounds are often stated with many constants from different steps of the proof. For reader convenience, we provide the simplified version of our bound in Theorem 1. The proof, details (e.g., the constants), and discussions about the assumptions are provided in Appendix A. We begin with a few assumptions before stating our bound.

Assumption 1. For any sample $\tilde{\mathbf{X}} = (Y, \mathbf{X}) \sim P_{\tilde{\mathbf{X}}}$, $\tilde{\mathbf{X}}$ has bounded ℓ_2 norm s.t. $\|\tilde{\mathbf{X}}\|_2 \leq B$, for some $B > 0$.

Assumption 2. The loss function $\mathcal{L}(f_\Theta) = \|f_\Theta(\tilde{\mathbf{X}}) - \tilde{\mathbf{X}}\|^2$ is sub-Gaussian under the distribution $P_{\tilde{\mathbf{X}}}$ with a variance factor s^2 s.t. $\forall t > 0, \mathbb{E}_{P_{\tilde{\mathbf{X}}}} \left[\exp \left(t(\mathcal{L}(f_\Theta) - \mathcal{L}_P(f_\Theta)) \right) \right] \leq \exp \left(\frac{t^2 s^2}{2} \right)$.

Theorem 1. Let $f_\Theta : \tilde{\mathcal{X}} \rightarrow \tilde{\mathcal{X}}$ be a M -layer ReLU feed-forward network with layer size h , and each of its weight matrices has the spectral norm bounded by κ . Then, under Assumptions 1 and 2, for any $\delta, \gamma > 0$, with probability $1 - \delta$ over a training set of N i.i.d samples, for any Θ in (4), we have:

$$\mathcal{L}_P(f_\Theta) \leq 4\mathcal{L}_N(f_\Theta) + \frac{1}{N} \left[\mathcal{R}_{\Theta_1} + C_1(\mathcal{V}_{\Theta_1} + \mathcal{V}_{\Theta_2}) + \log \left(\frac{8}{\delta} \right) \right] + C_3 \quad (8)$$

where $\mathcal{L}_P(f_\Theta)$ is the expected reconstruction loss of $\tilde{\mathbf{X}}$ under $P_{\tilde{\mathbf{X}}}$, $\mathcal{L}_N(f_\Theta)$, \mathcal{V}_{Θ_1} and \mathcal{R}_{Θ_1} are defined in (6-7), \mathcal{V}_{Θ_2} is the ℓ_2 norm of the network weights in the output and shared hidden layers, and C_1 and C_2 are some constants depending on γ, d, h, B, s and M .

The statistical properties of the reconstruction loss in learning linear DAGs, e.g. $\mathcal{L}_{\mathbf{W}} = \frac{1}{N} \|\tilde{\mathbf{X}} - \mathbf{W}\tilde{\mathbf{X}}\|_F^2$, have been well studied in the literature: the loss minimizer provably recovers a true DAG with high probability on finite-samples, and hence is consistent for both Gaussian SEM [47] and non-Gaussian SEM [48, 49]. Note also that the regularizer $\mathcal{R}_{\mathbf{W}}$ or \mathcal{R}_{Θ_1} are not a part of the results in [47, 48, 49]. However, the works of [37, 38] empirically show that using $\mathcal{R}_{\mathbf{W}}$ or \mathcal{R}_{Θ_1} on top of the reconstruction loss leads to more efficient and more accurate DAG learning than existing approaches. Our theoretical result on the reconstruction loss explains the benefit of $\mathcal{R}_{\mathbf{W}}$ or \mathcal{R}_{Θ_1} for the generalization performance of predicting Y . This provides theoretical support for our CASTLE regularizer in supervised learning. However, the objectives of DAG discovery, e.g., identifying the Markov Blanket of Y , is beyond the scope of our analysis.

The bound in (8) justifies \mathcal{R}_{Θ_1} in general, including linear or nonlinear cases, if the underlying distribution $P_{\tilde{\mathbf{X}}}$ is factorized according to some causal DAG. We note that the expected loss $\mathcal{L}_P(f_\Theta)$ is upper bounded by the empirical loss $\mathcal{L}_N(f_\Theta)$, \mathcal{V}_{Θ_1} , \mathcal{V}_{Θ_2} and \mathcal{R}_{Θ_1} which measures how close (via acyclicity constraint) the model is to a DAG. From (8) it is obvious that not minimizing \mathcal{R}_{Θ_1} is an acceptable strategy asymptotically or in the large samples limit (large N) because \mathcal{R}_{Θ_1}/N becomes negligible. This aligns with the consistency theory in [47, 48, 49] for linear models. However for small N , a preferred strategy is to train a model f_Θ by minimizing $\mathcal{L}_N(f_\Theta)$ and \mathcal{R}_{Θ_1} jointly. This would be trivial because the samples are generated under the DAG structure in $P_{\tilde{\mathbf{X}}}$. Minimizing \mathcal{R}_{Θ_1} can decrease the upper bound of $\mathcal{L}_P(f_\Theta)$ in (8), improve the generalization performance of f_Θ , as well as facilitate the convergence of f_Θ to the true model.

If $P_{\tilde{\mathbf{X}}}$ does not correspond to any causal DAG, such as image data, then there will be a trade-off between minimizing \mathcal{R}_{Θ_1} and $\mathcal{L}_N(f_\Theta)$. In this case, \mathcal{R}_{Θ_1} becomes harder to minimize, and generalization may not benefit from adding CASTLE. However, this is a rare case since causal structure exists in most datasets inherently. Our experiments demonstrate that CASTLE regularization outperforms popular regularizers on a variety of datasets in the next section.

4 Experiments

In this section, we empirically evaluate CASTLE as a regularization method for improving generalization performance. We present our benchmark methods and training architecture, followed by our synthetic and publicly available data results.

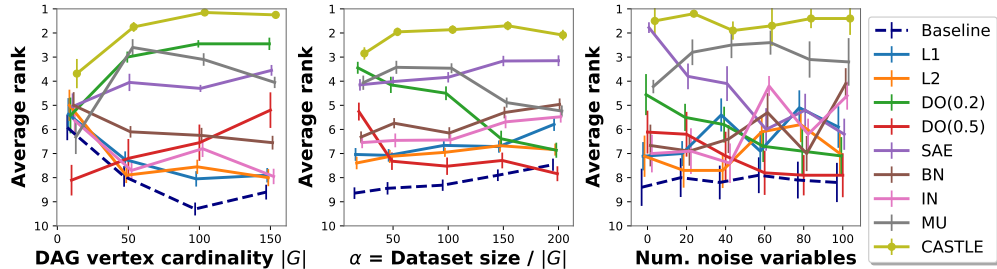


Figure 3: Experiments on synthetic data. The y -axis is the average rank (\pm standard deviation) of each regularizer on the test set over each synthetic DAG. We show the average rank as we increase the number of features or vertex cardinality $|G|$ (**left**), increase the dataset size normalized by the vertex cardinality $|G|$ (**center**), and as we increase the number of noise (neighborless) variables (**right**).

Benchmarks. We benchmark CASTLE against common regularizers that include: early stopping (Baseline) [31], L1 [29], L2 [30], dropout [3] with drop rate of 20% and 50% denoted as DO(0.2) and DO(0.5) respectively, SAE [12], batch normalization (BN) [33], data augmentation or input noise (IN) [2], and MixUp (MU) [35], in no particular order. For each regularizer with tunable hyperparameters we performed a standard grid search. For the weight decay regularizers L1 and L2 we searched for $\lambda_{\ell_p} \in \{0.1, 0.01, 0.001\}$, and for input noise we use a Gaussian noise with mean of 0 and standard deviation $\sigma \in \{0.1, 0.01, 0.01\}$. L1 and L2 were applied at every dense layer. BN and DO were applied after every dense layer and active only during training. Because each regularization method converges at different rates, we use early stopping on a validation set to terminate each benchmark training, which we refer to as our Baseline.

Network architecture and training. We implemented CASTLE in Tensorflow². Our proposed architecture is comprised of $d + 1$ sub-networks with shared hidden layers, as shown in Figure 2. In the linear case, $\mathcal{V}_{\mathbf{W}}$ is the ℓ_1 norm of \mathbf{W} . In the nonlinear case, \mathcal{V}_{Θ_1} is the ℓ_1 norm of the input weight matrices \mathbf{W}_1^k , $k \in [d + 1]$. To make a clear comparison with L2 regularization, we exclude the capacity term \mathcal{V}_{Θ_2} from CASTLE, although it is a part of our generalization bound in (8). Since we predict the target variable as our primary task, we benchmark CASTLE against this common network architecture. Specifically, we use a network with two hidden layers of $d + 1$ neurons with ReLU activation. Each benchmark method is initialized and seeded identically with the same random weights. For dataset preprocessing, all continuous variables are standardized with a mean of 0 and a variance of 1. Each model is trained using the Adam optimizer with a learning rate of 0.001 for up to a maximum of 200 epochs. An early stopping regime halts training with a patience of 30 epochs.

4.1 Regularization on Synthetic Data

Synthetic data generation. Given a DAG G , we generate functional relationships between each variable and its respective parent(s) with additive Gaussian noise applied to each variable with a mean of 0 and variance of 1. In the linear case, each variable is equal to the sum of its parents plus noise. For the nonlinear case, each variable is equal to the sum of the sigmoid of its parents plus noise. We provide further details on our synthetic DGP and pseudocode in Appendix B. Consider Table 2, using our nonlinear DGP we generated 1000 test samples according to the DAG in Figure 1. We then used 10-fold cross-validation to train and validate each benchmark on varying training sets of size n . Each model was evaluated on the test set from weights saved at the lowest validation error. Table 2 shows that CASTLE improves over all experimental benchmarks. We present similar results for our linear experiments in Appendix B.

Table 2: Experiments on nonlinear synthetic data of size n generated according to Fig. 1 in terms of MSE (\pm standard deviation)

Regularizer	$n = 500$	$n = 1000$	$n = 5000$
Baseline	0.83 \pm 0.03	0.80 \pm 0.04	0.73 \pm 0.02
L1	0.81 \pm 0.05	0.79 \pm 0.03	0.71 \pm 0.02
L2	0.81 \pm 0.05	0.77 \pm 0.02	0.71 \pm 0.01
DO(0.2)	0.80 \pm 0.04	0.79 \pm 0.01	0.70 \pm 0.02
DO(0.5)	0.79 \pm 0.02	0.78 \pm 0.04	0.70 \pm 0.02
SAE	0.79 \pm 0.03	0.77 \pm 0.04	0.69 \pm 0.02
BN	0.81 \pm 0.04	0.79 \pm 0.03	0.72 \pm 0.02
IN	0.82 \pm 0.05	0.78 \pm 0.04	0.71 \pm 0.02
MU	0.79 \pm 0.05	0.78 \pm 0.04	0.72 \pm 0.08
CASTLE	0.77 \pm 0.02	0.75 \pm 0.04	0.68 \pm 0.02

²Code is provided at <https://bitbucket.org/mvdschaar/mlforhealthlabpub>.

Table 3: Comparison of benchmark regularizers on regression and classification in terms of test MSE and AUROC (\pm standard deviation), respectively, for experiments on real datasets using 10-fold cross-validation. Bold denotes best performance. For conciseness we show only a subset of the benchmarks. The full version of this table is in Appendix C along with results on additional datasets.

Dataset	Baseline	L1	Dropout 0.2	SAE	Batch Norm	Input Noise	MixUp	CASTLE
Regression (MSE)								
BH	0.141 \pm 0.023	0.137 \pm 0.025	0.168 \pm 0.032	0.148 \pm 0.027	0.139 \pm 0.021	0.137 \pm 0.018	0.194 \pm 0.064	0.123 \pm 0.016
WQ	0.747 \pm 0.038	0.747 \pm 0.043	0.738 \pm 0.029	0.727 \pm 0.030	0.723 \pm 0.039	0.771 \pm 0.036	0.712 \pm 0.018	0.708 \pm 0.030
FB	0.758 \pm 1.017	0.663 \pm 0.796	0.429 \pm 0.449	0.372 \pm 0.168	0.705 \pm 0.396	0.609 \pm 0.511	0.385 \pm 0.208	0.246 \pm 0.153
BC	0.359 \pm 0.061	0.342 \pm 0.037	0.334 \pm 0.030	0.322 \pm 0.021	0.325 \pm 0.024	0.319 \pm 0.022	0.322 \pm 0.030	0.318 \pm 0.036
SP	0.416 \pm 0.108	0.421 \pm 0.181	0.285 \pm 0.042	0.228 \pm 0.022	0.318 \pm 0.062	0.389 \pm 0.095	0.267 \pm 0.072	0.200 \pm 0.020
CM	0.536 \pm 0.103	0.574 \pm 0.125	0.327 \pm 0.025	0.387 \pm 0.034	0.470 \pm 0.047	0.495 \pm 0.081	0.376 \pm 0.030	0.326 \pm 0.031
Classification (AUROC)								
CC	0.764 \pm 0.009	0.766 \pm 0.007	0.776 \pm 0.009	0.774 \pm 0.012	0.773 \pm 0.009	0.772 \pm 0.012	0.778 \pm 0.009	0.787 \pm 0.007
PD	0.799 \pm 0.008	0.793 \pm 0.013	0.797 \pm 0.010	0.796 \pm 0.010	0.773 \pm 0.024	0.796 \pm 0.013	0.802 \pm 0.016	0.817 \pm 0.004
BC	0.721 \pm 0.018	0.726 \pm 0.011	0.718 \pm 0.024	0.605 \pm 0.068	0.727 \pm 0.012	0.722 \pm 0.026	0.700 \pm 0.055	0.731 \pm 0.010
LV	0.559 \pm 0.061	0.594 \pm 0.020	0.579 \pm 0.053	0.542 \pm 0.095	0.583 \pm 0.026	0.597 \pm 0.041	0.553 \pm 0.092	0.595 \pm 0.032
SH	0.915 \pm 0.015	0.921 \pm 0.006	0.922 \pm 0.017	0.701 \pm 0.205	0.913 \pm 0.013	0.922 \pm 0.005	0.921 \pm 0.005	0.929 \pm 0.007
RP	0.782 \pm 0.071	0.801 \pm 0.013	0.743 \pm 0.052	0.774 \pm 0.103	0.802 \pm 0.018	0.796 \pm 0.009	0.730 \pm 0.043	0.814 \pm 0.014

Dissecting CASTLE. In the synthetic environment, we know the causal relationships with certainty. We analyze three aspects of CASTLE regularization using synthetic data. Because we are comparing across randomly simulated DAGs with differing functional relationships, the magnitude of regression testing error will vary between runs. We examine the model performance in terms of each model’s average rank over each fold to normalize this. If we have r regularizers, the best and worst possible rank is one and r , respectively (i.e., the higher the rank the better). We used 10-fold cross-validation to terminate model training and tested each model on a held-out test set of 1000 samples.

First, we examine the impact of increasing the feature size or DAG vertex cardinality $|G|$. We do this by randomly generating a DAG of size $|G| \in \{10, 50, 100, 150\}$ with $50|G|$ training samples. We repeat this ten times for each DAG cardinality. On the left-hand side of Fig. 3, CASTLE has the highest rank of all benchmarks and does not degrade with increasing $|G|$. Second, we analyze the impact of increasing dataset size. We randomly generate DAGs of size $|G| \in \{10, 50, 100, 150\}$, which we use to create datasets of $\alpha|G|$ samples, where $\alpha \in \{20, 50, 100, 150, 200\}$. We repeat this ten times for each dataset size. In the middle plot of Figure 3, we see that CASTLE has superior performance for all dataset sizes, and as expected, all benchmark methods (except for SAE) start to converge about the average rank at large data sizes ($\alpha = 200$). Third, we analyze our method’s sensitivity to noise variables, i.e., variables disconnected to the target variable in G . We randomly generate DAGs of size $|G| = 50$ to create datasets with $50|G|$ samples. We randomly add $v \in \{20i\}_{i=0}^5$ noise variables normally distributed with 0 mean and unit variance. We repeat this process for ten different DAG instantiations. The results on the right-hand side of Figure 3 show that our method is not sensitive to the existence of disconnected noise variables, whereas SAE performance degrades with the increase of uncorrelated input features. This highlights the benefit of target selection based on the DAG topology. In Appendix C, we provide an analysis of adjacency matrix weights that are learned under various random DAG configurations, e.g., target with parents, orphaned target, etc. There, we highlight CASTLE in comparison to SAE for target selection by showing that the adjacency matrix weights for noise variables are near zero. We also provide a sensitivity analysis on the parameter λ from (5) and results for additional experiments demonstrating that CASTLE does not reconstruct noisy (neighborless) variables in the underlying causal DAG.

4.2 Regularization on Real Data

We perform regression and classification experiments on a spectrum of publicly available datasets from [50] including Boston Housing (BH), Wine Quality (WQ), Facebook Metrics (FB), Bioconcentration (BC), Student Performance (SP), Community (CM), Contraception Choice (CC), Pima Diabetes (PD), Las Vegas Ratings (LV), Statlog Heart (SH), and Retinopathy (RP). For each dataset, we randomly reserve 20% of the samples for a testing set. We perform 10-fold cross-validation on the remaining 80%. As the results show in Table 3, CASTLE provides improved regularization across all datasets for both regression and classification tasks. Additionally, CASTLE consistently ranks as the top regularizer (graphically shown in Appendix C.3), with no definitive benchmark

method coming in as a consensus runner-up. This emphasizes the stability of CASTLE as a reliable regularizer. In Appendix C, we provide additional experiments on several other datasets, an ablation study highlighting our sources of gain, and real-world dataset statistics.

5 Conclusion

We have introduced CASTLE regularization, a novel regularization method that jointly learns the causal graph to improve generalization performance in comparison to existing capacity-based and reconstruction-based regularization methods. We used existing PAC-Bayes theory to provide a theoretical generalization bound for CASTLE. We have shown experimentally that CASTLE is insensitive to increasing feature dimensionality, dataset size, and uncorrelated noise variables. Furthermore, we have shown that CASTLE regularization improves performance on a plethora of real datasets and, in the worst case, never degrades performance. We hope that CASTLE will play a role as a general-purpose regularizer that can be leveraged by the entire machine learning community.

Broader Impact

One of the big challenges of machine learning, and deep learning in particular, is generalization to out-of-sample data. Regularization is necessary and used to prevent overfitting thereby promoting generalization. In this work, we have presented a novel regularization method inspired by causality. Since the applicability of our approach spans all problems where causal relationships exist between variables, there are countless beneficiaries of our research. Apart from the general machine learning community, the beneficiaries of our research include practitioners in the social sciences (sociology, psychology, etc.), natural sciences (physics, biology, etc.), and healthcare among countless others. These fields have already been exploiting causality for some time and serve as a natural launch-pad for deploying and leveraging CASTLE. With that said, our method does not immediately apply to certain architectures, such as CNNs, where causal relationships are ambiguous or perhaps non-existent.

Acknowledgments

This work was supported by GlaxoSmithKline (GSK), the US Office of Naval Research (ONR), and the National Science Foundation (NSF): grant numbers 1407712, 1462245, 1524417, 1533983, 1722516. We thank all reviewers for their generous comments and suggestions.

References

- [1] Larry S. Yaeger, Richard F. Lyon, and Brandyn J. Webb. Effective training of a neural network character classifier for word recognition. In M. C. Mozer, M. I. Jordan, and T. Petsche, editors, *Advances in Neural Information Processing Systems 9*, pages 807–816. MIT Press, 1997.
- [2] Alex Krizhevsky, Ilya Sutskever, and Geoffrey E. Hinton. Imagenet classification with deep convolutional neural networks. In *Proceedings of the 25th International Conference on Neural Information Processing Systems - Volume 1*, NIPS’12, page 1097–1105, Red Hook, NY, USA, 2012. Curran Associates Inc.
- [3] Geoffrey E. Hinton, Nitish Srivastava, Alex Krizhevsky, Ilya Sutskever, and Ruslan Salakhutdinov. Improving neural networks by preventing co-adaptation of feature detectors. *ArXiv*, abs/1207.0580, 2012.
- [4] Stefan Wager, Sida Wang, and Percy Liang. Dropout training as adaptive regularization. *Advances in Neural Information Processing Systems*, 07 2013.
- [5] Nitish Srivastava, Geoffrey Hinton, Alex Krizhevsky, Ilya Sutskever, and Ruslan Salakhutdinov. Dropout: A simple way to prevent neural networks from overfitting. *Journal of Machine Learning Research*, 15(56):1929–1958, 2014.
- [6] Sebastian Lunz, Ozan Öktem, and Carola-Bibiane Schönlieb. Adversarial regularizers in inverse problems. In S. Bengio, H. Wallach, H. Larochelle, K. Grauman, N. Cesa-Bianchi, and

- R. Garnett, editors, *Advances in Neural Information Processing Systems 31*, pages 8507–8516. Curran Associates, Inc., 2018.
- [7] Bin-Bin Gao, Chao Xing, Chen-Wei Xie, Jianxin Wu, and Xin Geng. Deep label distribution learning with label ambiguity. *IEEE Transactions on Image Processing*, 26:2825–2838, 04 2017.
- [8] Yoshua Bengio, Pascal Lamblin, Dan Popovici, and Hugo Larochelle. Greedy layer-wise training of deep networks. In *Proceedings of the 19th International Conference on Neural Information Processing Systems, NIPS’06*, page 153–160, Cambridge, MA, USA, 2006. MIT Press.
- [9] Marc’ Aurelio Ranzato and Martin Szummer. Semi-supervised learning of compact document representations with deep networks. In *Proceedings of the 25th International Conference on Machine Learning*, pages 792–799, 01 2008.
- [10] Tianyu He, Xu Tan, Yingce Xia, Di He, Tao Qin, Zhibo Chen, and Tie-Yan Liu. Layer-wise coordination between encoder and decoder for neural machine translation. In S. Bengio, H. Wallach, H. Larochelle, K. Grauman, N. Cesa-Bianchi, and R. Garnett, editors, *Advances in Neural Information Processing Systems 31*, pages 7944–7954. Curran Associates, Inc., 2018.
- [11] Pascal Vincent, Hugo Larochelle, Yoshua Bengio, and Pierre-Antoine Manzagol. Extracting and composing robust features with denoising autoencoders. In *Proceedings of the 25th international conference on Machine learning*, pages 1096–1103. ACM, 2008.
- [12] Lei Le, Andrew Patterson, and Martha White. Supervised autoencoders: Improving generalization performance with unsupervised regularizers. In *Advances in Neural Information Processing Systems*, pages 107–117, 2018.
- [13] Shengyu Zhu and Zhitang Chen. Causal discovery with reinforcement learning. *CoRR*, abs/1906.04477, 2019.
- [14] Ruichu Cai, Feng Xie, Clark Glymour, Zhifeng Hao, and Kun Zhang. Triad constraints for learning causal structure of latent variables. In *Advances in Neural Information Processing Systems 32*, pages 12883–12892. Curran Associates, Inc., 2019.
- [15] Uri Shalit, Fredrik D Johansson, and David Sontag. Estimating individual treatment effect: generalization bounds and algorithms. In *Proceedings of the 34th International Conference on Machine Learning-Volume 70*, pages 3076–3085. JMLR. org, 2017.
- [16] Ahmed Alaa and Mihaela van der Schaar. Validating causal inference models via influence functions. In Kamalika Chaudhuri and Ruslan Salakhutdinov, editors, *Proceedings of the 36th International Conference on Machine Learning*, volume 97 of *Proceedings of Machine Learning Research*, pages 191–201, Long Beach, California, USA, 09–15 Jun 2019. PMLR.
- [17] Patrick Schwab and Walter Karlen. Cxplain: Causal explanations for model interpretation under uncertainty. In *Advances in Neural Information Processing Systems 32*, pages 10220–10230. Curran Associates, Inc., 2019.
- [18] Kun Zhang, Bernhard Schölkopf, Krikamol Muandet, and Zhikun Wang. Domain adaptation under target and conditional shift. In Sanjoy Dasgupta and David McAllester, editors, *Proceedings of the 30th International Conference on Machine Learning (ICML)*, volume 28 of *Proceedings of Machine Learning Research*, pages 819–827, 2013.
- [19] Jonas Peters, Peter Bühlmann, and Nicolai Meinshausen. Causal inference by using invariant prediction: identification and confidence intervals. *Journal of the Royal Statistical Society: Series B (Statistical Methodology)*, 78(5):947–1012, 2016.
- [20] Sara Magliacane et al. Domain adaptation by using causal inference to predict invariant conditional distributions. In S. Bengio et al., editors, *Advances in Neural Information Processing Systems 31*, pages 10846–10856. Curran Associates, Inc., 2018.
- [21] Mateo Rojas-Carulla, Bernhard Schölkopf, Richard Turner, and Jonas Peters. Invariant models for causal transfer learning. *Journal of Machine Learning Research*, 19(36):1–34, 2018.

- [22] Bernhard Schölkopf, Dominik Janzing, Jonas Peters, Eleni Sgouritsa, Kun Zhang, and Joris Mooij. On causal and anticausal learning. *Proceedings of the 29th International Conference on Machine Learning, ICML 2012*, 2, 06 2012.
- [23] Mohammad Taha Bahadori, Krzysztof Chalupka, Edward Choi, Robert Chen, Walter F. Stewart, and Jimeng Sun. Causal regularization. *CoRR*, abs/1702.02604, 2017.
- [24] Dominik Rothenhausler, Nicolai Meinshausen, Peter Buhlmann, and Jonas Peters. Anchor regression: heterogeneous data meet causality. *CoRR*, abs/1801.06229, 2018.
- [25] Dominik Janzing. Causal regularization. In *Advances in Neural Information Processing Systems 32*, pages 12704–12714. Curran Associates, Inc., 2019.
- [26] Bernhard Schölkopf, Dominik Janzing, Jonas Peters, Eleni Sgouritsa, Kun Zhang, and Joris Mooij. On causal and anticausal learning. In *Proceedings of the 29th International Conference on Machine Learning, ICML’12*, page 459–466, Madison, WI, USA, 2012. Omnipress.
- [27] David Lopez-Paz, Robert Nishihara, Soumith Chintala, Bernhard Schölkopf, and Leon Bottou. Discovering causal signals in images. In *The IEEE Conference on Computer Vision and Pattern Recognition (CVPR)*, July 2017.
- [28] Dominik Janzing and Bernhard Schölkopf. Semi-supervised interpolation in an anticausal learning scenario. *J. Mach. Learn. Res.*, 16(1):1923–1948, January 2015.
- [29] Robert Tibshirani. Regression shrinkage and selection via the lasso. *Journal of the Royal Statistical Society: Series B (Methodological)*, 58(1):267–288, 1996.
- [30] Arthur Hoerl and Robert Kennard. Ridge regression: Biased estimation for nonorthogonal problems. *Technometrics*, 12:55–67, 04 2012.
- [31] Ian Goodfellow, Yoshua Bengio, and Aaron Courville. *Deep Learning*. MIT Press, 2016.
- [32] Razvan Pascanu, Tomas Mikolov, and Yoshua Bengio. On the difficulty of training recurrent neural networks. In *ICML*, 2012.
- [33] Sergey Ioffe and Christian Szegedy. Batch normalization: Accelerating deep network training by reducing internal covariate shift. In *Proceedings of the 32nd International Conference on Machine Learning - Volume 37, ICML’15*, page 448–456. JMLR.org, 2015.
- [34] Hyeonwoo Noh, Tackgeun You, Jonghwan Mun, and Bohyung Han. Regularizing deep neural networks by noise: Its interpretation and optimization. In *Proceedings of the 31st International Conference on Neural Information Processing Systems, NIPS’17*, page 5115–5124, Red Hook, NY, USA, 2017. Curran Associates Inc.
- [35] Hongyi Zhang, Moustapha Cisse, Yann Dauphin, and David Lopez-Paz. mixup: Beyond empirical risk minimization. *Proceedings of the 6th International Conference on Learning Representations (ICLR)*, 2018.
- [36] Krzysztof Chalupka, Frederick Eberhardt, and Pietro Perona. Estimating causal direction and confounding of two discrete variables. *arXiv preprint arXiv:1611.01504*, 2016.
- [37] Xun Zheng, Bryon Aragam, Pradeep Ravikumar, and Eric P. Xing. DAGs with NO TEARS: Continuous Optimization for Structure Learning. In *Advances in Neural Information Processing Systems*, 2018.
- [38] Xun Zheng, Chen Dan, Bryon Aragam, Pradeep Ravikumar, and Eric P Xing. Learning sparse nonparametric dags. *arXiv preprint arXiv:1909.13189*, 2019.
- [39] Sébastien Lachapelle, Philippe Brouillard, Tristan Deleu, and Simon Lacoste-Julien. Gradient-based neural DAG learning. In *Proceedings of the 8th International Conference on Learning Representations (ICLR)*, 2020.
- [40] J. Pearl. *Causality*. Causality: Models, Reasoning, and Inference. Cambridge Univ. Press, 2009.

- [41] Andreas Maurer, Massimiliano Pontil, and Bernardino Romera-Paredes. The benefit of multitask representation learning. *The Journal of Machine Learning Research*, 17(1):2853–2884, 2016.
- [42] John Langford and John Shawe-Taylor. Pac-bayes & margins. In *Advances in neural information processing systems*, pages 439–446, 2003.
- [43] John Shawe-Taylor and Robert C Williamson. A pac analysis of a bayesian estimator. In *Proceedings of the tenth annual conference on Computational learning theory*, pages 2–9, 1997.
- [44] David A. McAllester. Some pac-bayesian theorems. In *Machine Learning*, pages 230–234. ACM Press, 1998.
- [45] Behnam Neyshabur, Srinadh Bhojanapalli, and Nathan Srebro. A pac-bayesian approach to spectrally-normalized margin bounds for neural networks. *arXiv preprint arXiv:1707.09564*, 2017.
- [46] Vaishnavh Nagarajan and J Zico Kolter. Deterministic pac-bayesian generalization bounds for deep networks via generalizing noise-resilience. *arXiv preprint arXiv:1905.13344*, 2019.
- [47] Po-Ling Loh and Peter Bühlmann. High-dimensional learning of linear causal networks via inverse covariance estimation. *The Journal of Machine Learning Research*, 15(1):3065–3105, 2014.
- [48] Bryon Aragam, Arash A Amini, and Qing Zhou. Learning directed acyclic graphs with penalized neighbourhood regression. *arXiv preprint arXiv:1511.08963*, 2015.
- [49] Sara Van de Geer, Peter Bühlmann, et al. l_0 -penalized maximum likelihood for sparse directed acyclic graphs. *The Annals of Statistics*, 41(2):536–567, 2013.
- [50] Dheeru Dua and Casey Graff. UCI machine learning repository, 2020.
- [51] Nitish Shirish Keskar, Dheevatsa Mudigere, Jorge Nocedal, Mikhail Smelyanskiy, and Ping Tak Peter Tang. On large-batch training for deep learning: Generalization gap and sharp minima. *arXiv preprint arXiv:1609.04836*, 2016.
- [52] Pascal Germain, Francis Bach, Alexandre Lacoste, and Simon Lacoste-Julien. Pac-bayesian theory meets bayesian inference. In *Advances in Neural Information Processing Systems*, pages 1884–1892, 2016.
- [53] Joel A Tropp. User-friendly tail bounds for sums of random matrices. *Foundations of computational mathematics*, 12(4):389–434, 2012.

A Proof of Theorem 1

In this paper, we consider learning a causal DAG as our regularizer. We use a squared loss in our objective function. We find the sub-Gaussian assumption is more realistic than the bounded assumption because the squared loss function is usually unbounded but with strong tail decay property. We also assume our network weights have bounded spectral norm. Since a generalization bound considers all the models in the hypothesis class, the hypothesis class's capability should be restricted to upper bound the expected loss for all the regression models in the class. However, this assumption is not necessary for classification problems, since it is possible to normalize the network weight. The network still has the same prediction as before normalization due to the ReLU homogeneity.

Theorem 1. *Let $f_\Theta : \tilde{\mathcal{X}} \rightarrow \tilde{\mathcal{X}}$ be a M -layer ReLU feed-forward network with layer size h , and each of its weight matrices has the spectral norm bounded by κ . Then, under Assumptions 1 and 2, for any $\delta, \gamma > 0$, with probability $1 - \delta$ over a training set of N i.i.d samples, for any Θ in (4), we have:*

$$\mathcal{L}_P(f_\Theta) \leq 4\mathcal{L}_N(f_\Theta) + \frac{1}{N} \left[\mathcal{R}_{\Theta_1} + C_1(\mathcal{V}_{\Theta_1} + \mathcal{V}_{\Theta_2}) + \log\left(\frac{8}{\delta}\right) \right] + C_2 \quad (9)$$

where $\mathcal{L}_P(f_\Theta)$ is the expected reconstruction loss of $\tilde{\mathcal{X}}$ under $P_{\tilde{\mathcal{X}}}$, $\mathcal{L}_N(f_\Theta)$, \mathcal{V}_{Θ_1} and \mathcal{R}_{Θ_1} are defined in (6-7), \mathcal{V}_{Θ_2} is the l_2 norm of the network weights in the output and shared hidden layers, C_1 and C_2 are given as $C_1 = (\gamma^{-1} \zeta(d+1)\kappa^{M-1})^2$, $C_2 = s^2 + 6\gamma$, and $\zeta = MBe[2\log(2eh)]^{1/2}$.

Proof. Our proof consists of three steps: (1) We convert the existing PAC-Bayes bound for a randomized model f_{Θ_u} to a deterministic model f_Θ ; (2) We upper bound the KL divergence in the PAC-Bayes bound by the capability terms (i.e. the regularizers) of our model; (3) We discuss how to choose the constants in our bound to make our result universal.

Step 1. We let $\tilde{\Theta}_u$ denote the Θ in which we perturb each parameter by a random perturbation u drawn from some Gaussian distribution. We collect all the random perturbation into one vector \mathbf{u} , and $\mathbf{u} \sim N(\mathbf{0}, \sigma^2 I)$. We let Q_{Θ_u} denote the distribution of Θ_u , and P_{Θ_u} denote our prior on Θ_u . For $\mathcal{L}_N(f_{\Theta_u})$, we have

$$\begin{aligned} \mathbb{E}_{\mathbf{u}}[\mathcal{L}_N(f_{\Theta_u})] &= \mathbb{E}_{\mathbf{u}} \left[\frac{1}{N} \sum_{i=1}^N \|f_{\Theta_u}(\tilde{\mathbf{X}}_i) - f_\Theta(\tilde{\mathbf{X}}_i) + f_\Theta(\tilde{\mathbf{X}}_i) - \tilde{\mathbf{X}}_i\|^2 \right] \\ &= \mathbb{E}_{\mathbf{u}} \left[\frac{1}{N} \sum_{i=1}^N \|f_{\Theta_u}(\tilde{\mathbf{X}}_i) - f_\Theta(\tilde{\mathbf{X}}_i)\|^2 \right] + \frac{1}{N} \sum_{i=1}^N \|f_\Theta(\tilde{\mathbf{X}}_i) - \tilde{\mathbf{X}}_i\|^2 \\ &\quad + \mathbb{E}_{\mathbf{u}} \left[\frac{2}{N} \sum_{i=1}^N (f_{\Theta_u}(\tilde{\mathbf{X}}_i) - f_\Theta(\tilde{\mathbf{X}}_i))(f_\Theta(\tilde{\mathbf{X}}_i) - \tilde{\mathbf{X}}_i) \right] \\ &\leq \mathbb{E}_{\mathbf{u}} \left[\frac{1}{N} \sum_{i=1}^N \|f_{\Theta_u}(\tilde{\mathbf{X}}_i) - f_\Theta(\tilde{\mathbf{X}}_i)\|^2 \right] + \frac{1}{N} \sum_{i=1}^N \|f_\Theta(\tilde{\mathbf{X}}_i) - \tilde{\mathbf{X}}_i\|^2 \\ &\quad + \mathbb{E}_{\mathbf{u}} \left[\frac{1}{N} \sum_{i=1}^N \|f_{\Theta_u}(\tilde{\mathbf{X}}_i) - f_\Theta(\tilde{\mathbf{X}}_i)\|^2 \right] + \frac{1}{N} \sum_{i=1}^N \|f_\Theta(\tilde{\mathbf{X}}_i) - \tilde{\mathbf{X}}_i\|^2 \\ &\leq 2\gamma + 2\mathcal{L}_N(f_\Theta) \end{aligned} \quad (10)$$

Similarly, we have

$$\begin{aligned} \mathcal{L}_P(f_\Theta) &= \mathbb{E}_P \mathbb{E}_{\mathbf{u}} \left[\|f_\Theta(\tilde{\mathbf{X}}) - f_{\Theta_u}(\tilde{\mathbf{X}}) + f_{\Theta_u}(\tilde{\mathbf{X}}) - \tilde{\mathbf{X}}\|^2 \right] \\ &\leq 2\gamma + 2\mathbb{E}_{\mathbf{u}}[\mathcal{L}_P(f_{\Theta_u})] \end{aligned} \quad (11)$$

where we let γ be a constant such that $\max_{\tilde{\mathbf{X}} \in \mathcal{X}} \mathbb{E}_{\mathbf{u}}[\|f_{\Theta_u}(\tilde{\mathbf{X}}) - f_\Theta(\tilde{\mathbf{X}})\|^2] \leq \gamma$. It is the upper bound for the maximum expected change of the network output when the weights are perturbed, thereby the network's sharpness as defined in [51].

Using the Corollary 4 in [52] and Lemma 1 in [45], we have the following PAC Bayes bound for the randomized model f_{Θ_u} . Given a prior distribution P_{Θ_u} over the set of predictors that is independent

of the training data, the PAC-Bayes theorem states that with probability at least $1 - \delta$, over N i.i.d training samples, the expected error of f_{Θ_u} can be bounded as follows,

$$\mathbb{E}_u[\mathcal{L}_P(f_{\Theta_u})] \leq \mathbb{E}_u[\mathcal{L}_N(f_{\Theta_u})] + \frac{1}{N} \left[2 \text{KL}(Q_{\Theta_u} \| P_{\Theta_u}) + \log\left(\frac{8}{\delta}\right) \right] + \frac{1}{2} s^2 \quad (12)$$

If we upper bound $\mathbb{E}_u[\mathcal{L}_P(f_{\Theta_u})]$ in (11) by (12), we have

$$\begin{aligned} \mathcal{L}_P(f_{\Theta}) &\leq 2\gamma + 2\mathbb{E}_u[\mathcal{L}_N(f_{\Theta_u})] + \frac{2}{N} \left[2 \text{KL}(Q_{\Theta_u} \| P_{\Theta_u}) + \log\left(\frac{8}{\delta}\right) \right] + s^2 \\ &\leq 4\mathcal{L}_N(f_{\Theta}) + \frac{2}{N} \left[2 \text{KL}(Q_{\Theta_u} \| P_{\Theta_u}) + \log\left(\frac{8}{\delta}\right) \right] + C_2 \end{aligned} \quad (13)$$

where the last inequality is achieved by (10), and $C_2 = s^2 + 6\gamma$.

Step 2. For convenience, we restate the parameter set Θ in (4) here,

$$\Theta_1 = \{\mathbf{W}_1^k\}_{k=1}^{d+1}, \quad \Theta = \Theta_1 \cup \{\mathbf{W}_m\}_{m=2}^M$$

Now we write the distribution Q_{Θ_u} and P_{Θ_u} explicitly. Without loss of generality, we assume Q_{Θ_u} and P_{Θ_u} have the same standard deviation σ^2 . First, Q_{Θ_u} is given as $Q_{\Theta_u} = Q_{\Theta_u}^{(1)} Q_{\Theta_u}^{(2)}$, where $Q_{\Theta_u}^{(1)} = N(z_{\Theta_u,1}; z_{\Theta_1}, 1)$, and

$$Q_{\Theta_u}^{(2)} = \prod_{k=1}^{d+1} N(\mathbf{W}_{u,1}^k; \mathbf{W}_1^k, \sigma^2 I) \prod_{m=2}^M N(\mathbf{W}_{u,m}; \mathbf{W}_m, \sigma^2 I).$$

And P_{Θ} is given as $P_{\Theta_u} = P_{\Theta_u}^{(1)} P_{\Theta_u}^{(2)}$, where $P_{\Theta_u}^{(1)} = N(z_{\Theta_u,1}; d+1, 1)$, and

$$P_{\Theta_u}^{(2)} = \prod_{k=1}^{d+1} N(\mathbf{W}_{u,1}^k; \mathbf{0}, \sigma^2 I) \prod_{m=2}^M N(\mathbf{W}_{u,m}; \mathbf{0}, \sigma^2 I).$$

The variable $z_{\Theta_u,1}$ is given as,

$$z_{\Theta_u,1} = \text{Tr}(e^{\mathbf{M}_u \odot \mathbf{M}_u})$$

where \mathbf{M}_u is a $(d+1) \times (d+1)$ matrix such that $[\mathbf{M}_u]_{k,j}$ is the ℓ_2 -norm of the k -th row of the matrix $\mathbf{W}_{u,1}^j$. The variable z_{Θ_1} is defined in the same way as $z_{\Theta_u,1}$ but on the parameters without perturbations. Here, we use Gaussian distributions for z 's for simplicity in our deterministic model. Formally, in Bayesian inference, we may consider using truncated normal or exponential priors for z 's since we know $z_{\Theta_u,1} = \text{Tr}(I) + \text{Tr}(\mathbf{M}_u \odot \mathbf{M}_u) + \dots \geq d+1$ using the power series of matrix exponential and the fact that each element of \mathbf{M}_u is non-negative. Now we upper bound the KL divergence as follows,

$$\begin{aligned} \text{KL}(Q_{\Theta_u} \| P_{\Theta_u}) &= \int Q_{\Theta_u}^{(1)} Q_{\Theta_u}^{(2)} \log\left(\frac{Q_{\Theta_u}^{(1)} Q_{\Theta_u}^{(2)}}{P_{\Theta_u}^{(1)} P_{\Theta_u}^{(2)}}\right) d\Theta_u \\ &= \int Q_{\Theta_u}^{(1)} Q_{\Theta_u}^{(2)} \log\left(\frac{Q_{\Theta_u}^{(1)}}{P_{\Theta_u}^{(1)}}\right) d\Theta_u + \int Q_{\Theta_u}^{(1)} Q_{\Theta_u}^{(2)} \log\left(\frac{Q_{\Theta_u}^{(2)}}{P_{\Theta_u}^{(2)}}\right) d\Theta_u \\ &\leq \int Q_{\Theta_u}^{(1)} \log\left(\frac{Q_{\Theta_u}^{(1)}}{P_{\Theta_u}^{(1)}}\right) d\Theta_u + \int Q_{\Theta_u}^{(2)} \log\left(\frac{Q_{\Theta_u}^{(2)}}{P_{\Theta_u}^{(2)}}\right) d\Theta_u \\ &= \frac{1}{2} [z_{\Theta_1} - (d+1)]^2 + \frac{1}{2\sigma^2} \left(\sum_{k=1}^{d+1} \|\mathbf{W}_1^k\|_F^2 + \sum_{m=2}^M \|\mathbf{W}_m\|_F^2 \right) \\ &\leq \frac{1}{2} \mathcal{R}_{\theta_1} + \frac{1}{2\sigma^2} (\mathcal{V}_{\Theta_1} + \mathcal{V}_{\Theta_2}) \end{aligned} \quad (14)$$

where the last inequality is achieved using the fact that the Euclidean norm of any vector is bounded by its ℓ_1 -norm. Let $C_1 = \frac{1}{\sigma^2}$. Bounding the KL divergence in (13) with (14) gives that

$$\mathcal{L}_P(f_{\Theta}) \leq 4\mathcal{L}_N(f_{\Theta}) + \frac{2}{N} \left[\mathcal{R}_{\theta_1} + C_1 (\mathcal{V}_{\Theta_1} + \mathcal{V}_{\Theta_2}) + \log\left(\frac{8}{\delta}\right) \right] + C_2 \quad (15)$$

Step 3. Recall that γ is the upper bound for $\max_{\tilde{\mathbf{X}} \in \mathcal{X}} \mathbb{E}_u[\|f_{\Theta_u}(\tilde{\mathbf{X}}) - f_{\Theta}(\tilde{\mathbf{X}})\|^2]$, the expected maximum change of the network output when the weights are perturbed by $\mathbf{u} \sim N(\mathbf{0}, \sigma^2 I)$. We

now derive the constant γ based on σ^2 , the input upper bound B in Assumption 1. Our network uses ReLU activation functions in the hidden layers. The ReLU function $\phi(\cdot)$ is 1-Lipschitz. This proof is similar to Lemma 2 in [45]. Let $\|\cdot\|_2$ denote the spectral norm. We define Δ_k^{M-1} as the output difference in the last hidden layer:

$$\Delta_k^{M-1} = \left\| \phi(\cdots \phi(\phi(\tilde{\mathbf{X}}[\mathbf{W}_1^k + \mathbf{U}_1^k])[\mathbf{W}_2 + \mathbf{U}_2]) \cdots [\mathbf{W}_{M-1} + \mathbf{U}_{M-1}]) - \phi(\cdots \phi(\phi(\tilde{\mathbf{X}}\mathbf{W}_1^k)\mathbf{W}_2) \cdots \mathbf{W}_{M-1}) \right\|$$

We have

$$\begin{aligned} \Delta_k^M &= ([f_{\Theta}(\tilde{\mathbf{X}})]_k - [f_{\Theta_u}(\tilde{\mathbf{X}})]_k)^2 \\ &= \Delta_k^{M-1} [\|\mathbf{W}_M\|_2 + \|\mathbf{U}_M\|_2] + \|\tilde{\mathbf{X}}\| \|\mathbf{U}_M\|_2 \|\mathbf{W}_1^k\|_2 \prod_{m=2}^{M-1} \|\mathbf{W}_m\|_2 \\ &\leq (1 + \frac{1}{M}) \|\mathbf{W}_M\|_2 \Delta_k^{M-1} + \frac{\|\mathbf{U}_M\|_2}{\|\mathbf{W}_M\|_2} \|\tilde{\mathbf{X}}\| \|\mathbf{W}_1^k\|_2 \prod_{m=2}^M \|\mathbf{W}_m\|_2 \\ &\leq (1 + \frac{1}{M}) \|\mathbf{W}_M\|_2 \left((1 + \frac{1}{M}) \|\mathbf{W}_{M-1}\|_2 \Delta_k^{M-2} + \frac{\|\mathbf{U}_{M-1}\|_2}{\|\mathbf{W}_{M-1}\|_2} \|\tilde{\mathbf{X}}\| \|\mathbf{W}_1^k\|_2 \prod_{m=2}^{M-1} \|\mathbf{W}_m\|_2 \right) \\ &\quad + \frac{\|\mathbf{U}_M\|_2}{\|\mathbf{W}_M\|_2} \|\tilde{\mathbf{X}}\| \|\mathbf{W}_1^k\|_2 \prod_{m=2}^M \|\mathbf{W}_m\|_2 \\ &\leq (1 + \frac{1}{M})^2 \Delta_k^{M-2} \prod_{m=M-1}^M \|\mathbf{W}_m\|_2 + \sum_{m=0}^1 (1 + \frac{1}{M})^m \frac{\|\mathbf{U}_{M-m}\|_2}{\|\mathbf{W}_{M-m}\|_2} \|\tilde{\mathbf{X}}\| \|\mathbf{W}_1^k\|_2 \prod_{m=2}^M \|\mathbf{W}_m\|_2 \\ &\leq (1 + \frac{1}{M})^M \|\tilde{\mathbf{X}} - \tilde{\mathbf{X}}\| F_k + (1 + \frac{1}{M})^{M-1} \frac{\|\mathbf{U}_1^k\|_2}{\|\mathbf{W}_1^k\|_2} \|\tilde{\mathbf{X}}\| F_k \\ &\quad + \sum_{m=0}^{M-2} (1 + \frac{1}{M})^m \frac{\|\mathbf{U}_{M-m}\|_2}{\|\mathbf{W}_{M-m}\|_2} \|\tilde{\mathbf{X}}\| F_k \\ &\leq eBF_k \left(\frac{\|\mathbf{U}_1^k\|_2}{\|\mathbf{W}_1^k\|_2} + \sum_{m=2}^M \frac{\|\mathbf{U}_m\|_2}{\|\mathbf{W}_m\|_2} \right) \end{aligned}$$

where $F_k = \|\mathbf{W}_1^k\|_2 \prod_{m=2}^M \|\mathbf{W}_m\|_2$, the last inequality is achieved by $(1 + \frac{1}{m})^M \leq e$ for $m \leq M$, and $\|\tilde{\mathbf{X}}\| \leq B$ in Assumption 1. Then $\mathbb{E}_u[\|f_{\Theta_u}(\tilde{\mathbf{X}}) - f_{\Theta}(\tilde{\mathbf{X}})\|^2]$ is given as

$$\begin{aligned} \sum_{k=1}^{d+1} \mathbb{E}_u[\Delta_k^M] &\leq \sigma r e B \sum_{k=1}^{d+1} F_k \left(\|\mathbf{W}_1^k\|_2^{-1} + \sum_{m=2}^M \|\mathbf{W}_m\|_2^{-1} \right) \\ &\leq \sigma r e B \sum_{k=1}^{d+1} \left(\prod_{m=2}^M \|\mathbf{W}_m\|_2 + \sum_{m=2}^M \frac{F_k}{\|\mathbf{W}_m\|_2} \right) \\ &\leq \sigma r e B (d+1) M \kappa^{M-1} \end{aligned}$$

where $r = [2 \log(2eh)]^{1/2}$, and the first inequality is achieved bounding the spectral norm of the random matrices \mathbf{U} 's using random matrix theory (See Section 4.4 in [53]). Hence, setting $\sigma = (r e B (d+1) M \kappa^{M-1})^{-1} \gamma$, then we have

$$\max_{\tilde{\mathbf{X}} \in \mathcal{X}} \mathbb{E}_u[\|f_{\Theta_u}(\tilde{\mathbf{X}}) - f_{\Theta}(\tilde{\mathbf{X}})\|^2] < \gamma.$$

Given any ReLU network satisfying the Assumptions 1 and 2 and with bounded spectral norm on its weights, we can upper bound its expected loss using the network sharpness, measured by some perturbations on the network parameters. \square

B Synthetic details

In this section, we cover details regarding our synthetic data generation process and experiments. We first provide an overview of our data generation, and then we will cover a supplementary linear example.

B.1 Synthetic data generating process

Here we describe our synthetic data generation process in detail. We enumerated all nodes in G randomly. We generated random DAG instantiations with a randomly sampled branching factor up to the number of nodes in the DAG for our synthetic DAG generation. Edges were randomly added to the graph until either the branching factor was met or no more edges can be added without violating graphical acyclicity. We provide pseudocode for our synthetic DGP in Algorithm 1. For each random DAG in our experiment we randomly chose a σ between 0.3 and 1, and we set $\mu = 0$ and $w = 1$.

For our experiments in the main paper, we use the following settings. In the linear case, each variable is equal to the sum of its parents plus noise. For the nonlinear case, each variable is equal to the sum of the sigmoid function of each parent plus noise.

Algorithm 1 Synthetic Data Generating Process (DGP)

Input: A Graphical structure G , a mean μ , standard deviation σ , edge weights w , a dataset size n .
Output: A dataset according to G with n samples.
Function: `gen_data(G, μ, σ, w, n)`:
 $e \leftarrow$ edges of G
 $G_{sorted} \leftarrow$ `topological_graph_sort(G)`
 $ret \leftarrow$ empty list
for $node \in G$ **do**
 Append to $ret[node]$ a list of Gaussian (μ and σ) randomly sampled list of size n .
end for
for $node \in G_{sorted}$ **do**
 for $par \in \{parents(node)\}$ **do**
 $ret[node] += ret[par] * w(par, node)$, where $w(par, node)$ is the edge weight from par to $node$. Note that a non-linear function can be applied to $ret[par]$ to convert this into a non-linear data generator.
 end for
end for
return ret .

B.2 Experiments on linear toy example

Table 4: Comparison of benchmark regularizers in terms of MSE (\pm standard deviation) for linear synthetic datasets of size n generated according to Fig. 1 using 10-fold cross-validation. A held-out test set of 1000 samples was generated and used for evaluating each method. Bold denotes best performing regularizer.

Regularizer	$n = 500$	$n = 1000$	$n = 5000$	$n = 10000$	$n = 50000$
L1	1.413 \pm 0.091	1.210 \pm 0.045	1.051 \pm 0.009	1.022 \pm 0.005	1.004 \pm 0.006
L2	1.327 \pm 0.057	1.208 \pm 0.064	1.027 \pm 0.009	1.022 \pm 0.008	1.008 \pm 0.004
Dropout (0.2)	1.287 \pm 0.045	1.237 \pm 0.011	1.216 \pm 0.003	1.213 \pm 0.004	1.209 \pm 0.002
Dropout (0.5)	1.227 \pm 0.036	1.191 \pm 0.017	1.159 \pm 0.003	1.161 \pm 0.006	1.157 \pm 0.006
SAE	1.323 \pm 0.152	1.164 \pm 0.033	1.138 \pm 0.026	1.137 \pm 0.009	1.145 \pm 0.019
Batch Norm	1.470 \pm 0.056	1.320 \pm 0.055	1.095 \pm 0.020	1.044 \pm 0.009	1.018 \pm 0.009
Input Noise	1.340 \pm 0.068	1.268 \pm 0.034	1.089 \pm 0.020	1.049 \pm 0.011	1.017 \pm 0.009
MixUP	1.306 \pm 0.074	1.214 \pm 0.040	1.112 \pm 0.012	1.075 \pm 0.008	1.047 \pm 0.006
CASTLE	1.205 \pm 0.093	1.042 \pm 0.024	1.009 \pm 0.018	1.008 \pm 0.015	1.004 \pm 0.018

Using our linear method, we performed experiments on our toy example in Figure 1. We use the same experimental setup from the toy example in the main manuscript but with linear settings. Our

results are shown in Table 4, which demonstrates that CASTLE is the superior regularizer over all dataset sizes (similar to the nonlinear case).

C Supplementary experiments, details, and results

In this section, we provide additional experiments to supplement the main manuscript.

C.1 Sensitivity analysis and hyperparameter optimization

Before we present further results, we first provide a sensitivity analysis on λ from (5). We use our synthetic DAG to synthesize a random DAG with between 10 and 150 nodes. We generated 2000 test samples and a training set with between 1000 and 5000 samples. We repeated this 50 times. Using 10-fold cross-validation we show a sensitivity analysis over $\lambda \in \{0.01, 0.1, 1, 10, 100\}$ in Figure 4 in terms of average rank. We compare using average rank since each experimental run (random DAG) will vary significantly in the magnitude of errors. Based on these results, for all of our experiments in this paper we use $\lambda = 1$, i.e., $\log(\lambda) = 0$. After fixing λ , our model has only one hyperparameter β to tune. For β in (6), we performed a standard grid search for the hyperparameter $\beta \in \{0.001, 0.01, 0.1, 1\}$.

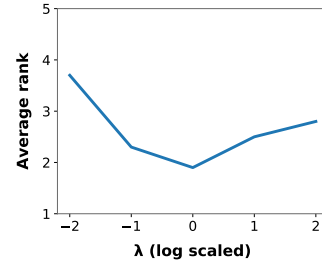


Figure 4: Sensitivity analysis on λ .

C.2 Scalability analysis

We perform an analysis of the scalability of CASTLE. Using our synthetic DAG and dataset generator, we synthesized datasets of 1000 samples. We used the same experimental setup used for the synthetic experiments. We present the computational timing results for CASTLE as we increase the number of input features on inference and training time in Figure 5. We see that the time to train 1000 samples grows exponentially with the feature size; however, the inference time remains linear as expected. Inference time on 1000 samples with 400 features takes approximately 2 seconds, while training time takes nearly 70 seconds. Computational time scales linearly with increasing the number of input samples. Experiments were conducted on an Ubuntu 18.04 OS using 6 Intel i7-6850K CPUs.

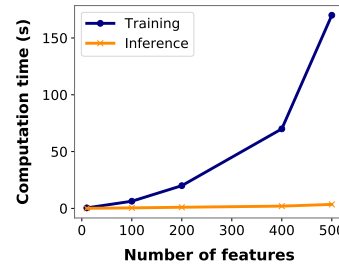


Figure 5: CASTLE scalability analysis

C.3 Additional results

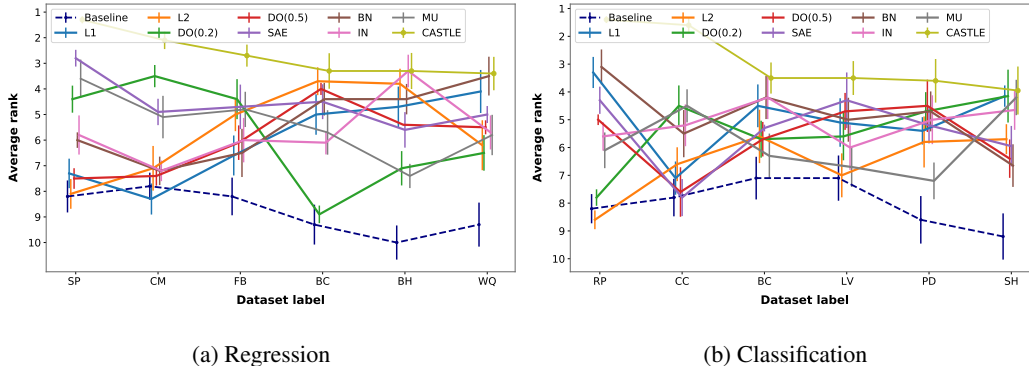


Figure 6: Comparison of CASTLE against benchmark regularization methods in terms of average rank across each fold (10-fold cross-validation) for regression (a) and classification (b) tasks. For clarity, we have sorted the datasets by average rank of CASTLE in decreasing order. In comparison to the other benchmarks, CASTLE maintains stable performance across datasets. Higher rank is better.

Table 5: Complete table of benchmark regularizers on regression in terms of test MSE (\pm standard deviation) for experiments on real datasets using 10-fold cross-validation. Bold denotes lowest test MSE. For readability we split the table into two.

\mathcal{D}	Baseline	L1	L2	Dropout 0.2	Dropout 0.5
BH	0.141 \pm 0.023	0.137 \pm 0.025	0.131 \pm 0.014	0.168 \pm 0.032	0.389 \pm 0.106
WQ	0.747 \pm 0.038	0.747 \pm 0.043	0.746 \pm 0.039	0.738 \pm 0.029	0.850 \pm 0.068
FB	0.758 \pm 1.017	0.663 \pm 0.796	1.341 \pm 1.069	0.429 \pm 0.449	0.597 \pm 0.313
BC	0.359 \pm 0.061	0.342 \pm 0.037	0.370 \pm 0.142	0.334 \pm 0.030	0.434 \pm 0.080
SP	0.416 \pm 0.108	0.421 \pm 0.181	0.550 \pm 0.291	0.285 \pm 0.042	0.482 \pm 0.128
CM	0.536 \pm 0.103	0.574 \pm 0.125	0.527 \pm 0.060	0.327 \pm 0.025	0.519 \pm 0.064
ME	0.885 \pm 0.056	0.878 \pm 0.062	0.935 \pm 0.060	0.729 \pm 0.032	0.710 \pm 0.022

\mathcal{D}	SAE	Batch Norm	Input Noise	MixUp	CASTLE
BH	0.148 \pm 0.027	0.139 \pm 0.021	0.137 \pm 0.018	0.194 \pm 0.064	0.123 \pm 0.016
WQ	0.727 \pm 0.030	0.723 \pm 0.039	0.771 \pm 0.036	0.712 \pm 0.018	0.708 \pm 0.030
FB	0.372 \pm 0.168	0.705 \pm 0.396	0.609 \pm 0.511	0.385 \pm 0.208	0.246 \pm 0.153
BC	0.322 \pm 0.021	0.325 \pm 0.024	0.319 \pm 0.022	0.322 \pm 0.030	0.318 \pm 0.036
SP	0.228 \pm 0.022	0.318 \pm 0.062	0.389 \pm 0.095	0.267 \pm 0.072	0.200 \pm 0.020
CM	0.387 \pm 0.034	0.470 \pm 0.047	0.495 \pm 0.081	0.376 \pm 0.030	0.326 \pm 0.031
ME	0.800 \pm 0.046	0.892 \pm 0.096	0.855 \pm 0.042	0.866 \pm 0.068	0.694 \pm 0.023

Table 6: Comparison of benchmark regularizers on classification in terms of test AUROC (\pm standard deviation) for experiments on real datasets using 10-fold cross-validation. Bold denotes highest test AUROC. For readability we split the table into two.

\mathcal{D}	Baseline	L1	L2	Dropout 0.2	Dropout 0.5
CC	0.764 \pm 0.009	0.766 \pm 0.007	0.768 \pm 0.010	0.776 \pm 0.009	0.756 \pm 0.023
PD	0.799 \pm 0.008	0.793 \pm 0.013	0.788 \pm 0.024	0.797 \pm 0.010	0.800 \pm 0.012
BC	0.721 \pm 0.018	0.726 \pm 0.011	0.712 \pm 0.045	0.713 \pm 0.022	0.718 \pm 0.024
LV	0.559 \pm 0.061	0.594 \pm 0.020	0.586 \pm 0.028	0.579 \pm 0.053	0.580 \pm 0.033
SH	0.915 \pm 0.015	0.921 \pm 0.006	0.919 \pm 0.011	0.922 \pm 0.017	0.914 \pm 0.010
RP	0.782 \pm 0.071	0.801 \pm 0.013	0.796 \pm 0.013	0.743 \pm 0.052	0.721 \pm 0.057
MG	0.644 \pm 0.109	0.675 \pm 0.114	0.647 \pm 0.134	0.628 \pm 0.081	0.679 \pm 0.090

\mathcal{D}	SAE	Batch Norm	Input Noise	MixUp	CASTLE
CC	0.774 \pm 0.012	0.773 \pm 0.009	0.772 \pm 0.012	0.778 \pm 0.009	0.787 \pm 0.007
PD	0.796 \pm 0.010	0.773 \pm 0.024	0.796 \pm 0.013	0.802 \pm 0.016	0.817 \pm 0.004
BC	0.605 \pm 0.068	0.727 \pm 0.012	0.722 \pm 0.026	0.700 \pm 0.055	0.731 \pm 0.010
LV	0.542 \pm 0.095	0.583 \pm 0.026	0.597 \pm 0.041	0.553 \pm 0.092	0.595 \pm 0.032
SH	0.701 \pm 0.205	0.913 \pm 0.013	0.922 \pm 0.005	0.921 \pm 0.005	0.929 \pm 0.007
RP	0.774 \pm 0.103	0.802 \pm 0.018	0.796 \pm 0.009	0.730 \pm 0.043	0.814 \pm 0.014
MG	0.597 \pm 0.135	0.672 \pm 0.072	0.671 \pm 0.138	0.685 \pm 0.081	0.731 \pm 0.036

In this subsection, we provide supplementary results on real data. In addition to the public datasets in the main paper, we provide experiments on some additional datasets. Specifically, we perform experiments on the Medical Expenditure Panel Survey (MEPS) [54]. This dataset contains samples from a broad survey of families and individuals, their medical providers, and employers across the US. MEPS is mainly concerned with collecting data related to health service utilization, frequency, cost, payment, and insurance coverage for Americans. For this dataset, we predicted health service utilization. We abbreviate MEPS as ME. We also provided additional experimentation on the Meta-analysis Global Group in Chronic heart failure database (MAGGIC), which holds data for 46,817 patients gathered from 30 independent clinical studies or registries [55]. For this dataset, we predicted mortality in patients with heart failure. We abbreviate MAGGIC as MG in Table 6.

We provide regression results on real data in Table 5. We provide classification results on real data in Table 6. Lastly, we depict the regression and classification results highlighted in the main paper in terms of rank. In Figure 6, we see that for both regression and classification, CASTLE performs the best, and there is no definitive runner-up benchmark method testifying to the stability of CASTLE as a reliable regularizer.

C.4 CASTLE ablation study

We provide an ablation study on CASTLE to understand the sources of gain of our methodology. Here we execute this experiment on our real datasets used in the main manuscript. We show the results of our ablation on our CASTLE regularizer to highlight our sources of gain in Table 7.

Table 7: Ablation study of CASTLE on real datasets to highlight sources of gain.

Dataset	$\mathcal{L}_N(f_\Theta) + \mathcal{V}_{\Theta_1}$	$\mathcal{R}_{\Theta_1} + \mathcal{V}_{\Theta_1}$	$\mathcal{L}_N(f_\Theta) + \mathcal{R}_{\Theta_1}$	$\mathcal{L}_N(f_\Theta) + \mathcal{R}_{\Theta_1} + \mathcal{V}_{\Theta_1}$
Regression (MSE)				
BH	0.162 ± 0.018	0.226 ± 0.158	0.174 ± 0.025	0.123 ± 0.016
WQ	0.711 ± 0.035	0.753 ± 0.013	0.713 ± 0.019	0.708 ± 0.030
FB	0.265 ± 0.045	0.327 ± 0.088	0.451 ± 0.032	0.246 ± 0.150
BC	0.362 ± 0.040	0.416 ± 0.009	0.373 ± 0.016	0.318 ± 0.036
SP	0.338 ± 0.181	0.212 ± 0.018	0.572 ± 0.340	0.200 ± 0.020
CM	0.347 ± 0.016	0.334 ± 0.007	0.478 ± 0.078	0.326 ± 0.031
Classification (AUROC)				
CC	0.778 ± 0.006	0.780 ± 0.008	0.768 ± 0.011	0.787 ± 0.007
PD	0.795 ± 0.012	0.792 ± 0.012	0.766 ± 0.012	0.817 ± 0.004
BC	0.712 ± 0.018	0.722 ± 0.008	0.712 ± 0.020	0.731 ± 0.010
LV	0.562 ± 0.033	0.586 ± 0.023	0.566 ± 0.027	0.595 ± 0.032
SH	0.895 ± 0.006	0.889 ± 0.011	0.890 ± 0.010	0.929 ± 0.007
RP	0.801 ± 0.012	0.802 ± 0.014	0.791 ± 0.012	0.814 ± 0.014

C.5 Weight characterization

In this subsection, we provide a characterization of the input weights that are learned during the CASTLE regularization. We performed synthetic experiments using the same setup for generating Figure 3. We investigated two different scenarios. In the first scenario, we randomly generated DAGs where the target must have causal parents. We examine the average weight value of the learned DAG adjacency matrix in comparison to the truth adjacency matrix for the parents, children, spouses, and siblings of the target variable. The results are shown in Figure 7. As expected, the results show that when causal parents exist, CASTLE prefers to predict in the causal direction, rather than the anti-causal direction (from children).

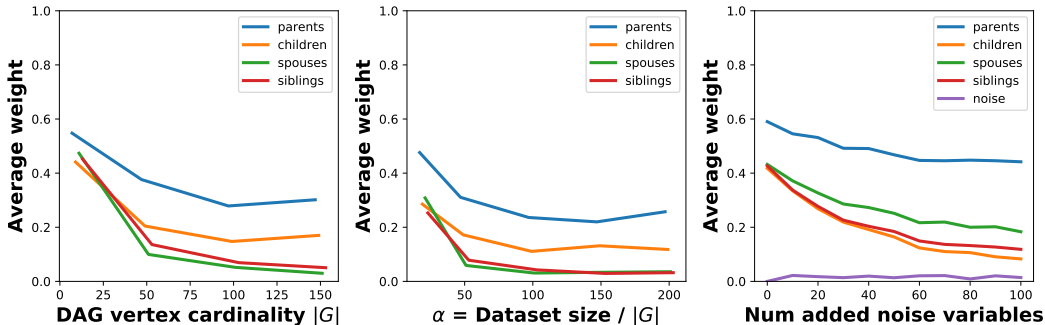


Figure 7: Weight values on synthetic data when true causal structure is known. Our method favors using the parents of the target when available.

As a secondary experiment, we ran the same sets of experiments, except for DAGs without parents of the target variable. Results are shown in Figure 8. The results show that when parents are not available that CASTLE finds the children as predictors rather than spouses. Note that in this experiment, there will be no siblings of the target variable, since the target variable has no parents.

Lastly, CASTLE does not reconstruct features that do not have causal neighbors in the discovered DAG. To highlight this, in our noise variable experiment, we show the average weighting of the input layers. In the right-most figures of Figure 7 and Figure 8, it is evident that the weighting is much lower (near zero) for the noise variables in comparison to the other variables in the DAG. This highlights the advantages of CASTLE over SAE, which naively reconstructs all variables.

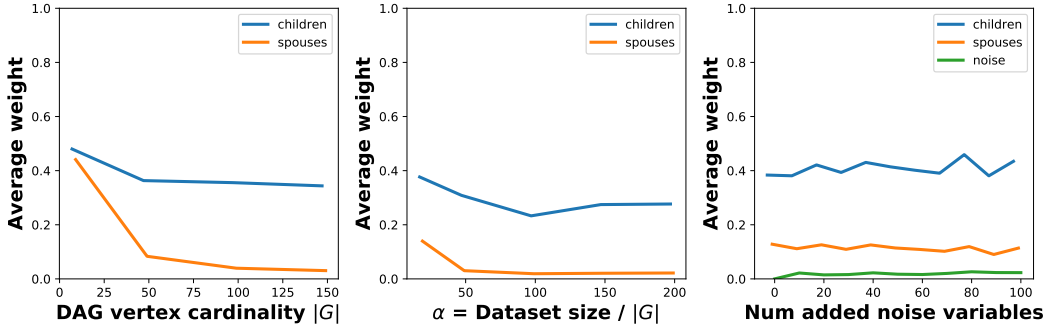


Figure 8: Weight values on synthetic data when true causal structure is known. This simulation was run with target variables not having any causal parents (and therefore no siblings as well). Our method favors using the children rather than spouses of the target.

C.6 Dataset details

In Table 8, we provide details of the real world datasets used in this paper. We demonstrated improved performance by CASTLE across a diverse collection of datasets in terms of sample and feature size.

Table 8: Real-world dataset details.

Dataset	Sample size	Feature size
Boston Housing (BH)	506	14
Wine Quality (WQ)	4894	12
Facebook Metrics (FB)	500	19
Bioconcentration (BC)	779	14
Student Performance (SP)	649	33
Community and Crime (CM)	1994	128
Contraceptive Choice (CC)	1472	9
Pima Diabetes (PD)	768	9
Las Vegas Ratings (LV)	504	20
Statlog Heart (SH)	270	13
Retinopathy (RP)	1151	20
Medical Expenditure Panel Survey (ME)	15786	139
Meta-analysis Global Group in Chronic (MG)	40367	33

Additional References for Appendices

- [54] Agency for Healthcare Research and Quality. Medical expenditure panel survey (meps), 2020.
- [55] Chih M. Wong et al. Heart failure in younger patients: the Meta-analysis Global Group in Chronic Heart Failure (MAGGIC). *European Heart Journal*, 35(39):2714–2721, 06 2014.